NJC

Accepted Manuscript

This article can be cited before page numbers have been issued, to do this please use: A. Colombo, E. Garoni, F. Nisic, S. Fantacci, G. Griffini, K. Kamada, D. Roberto and C. Dragonetti, *New J. Chem.*, 2018, DOI: 10.1039/C8NJ03216E.

ROYAL SOCIETY OF CHEMISTRY

rsc.li/njc

Journal Name

ROYAL SOCIETY OF CHEMISTRY View Article Online
DOI: 10.1039/C8NJ03216E

ARTICLE

Perylenetetracarboxy-3,4:9,10-diimide derivatives with large two-photon absorption activity

Received 00th January 20xx,
Accepted 00th January 20xx

DOI: 10.1039/x0xx00000x

www.rsc.org/

Eleonora Garoni,[a,b] Filippo Nisic,[a] Alessia Colombo,[a,*] Simona Fantacci,[c,*] Gianmarco Griffini,[d] Kenji Kamada [b,*] Dominique Roberto,[a] Claudia Dragonetti[a]

Three new perylenetetracarboxy-3,4:9,10-diimides, bearing 2,6-diisopropylphenyl groups at the imide positions and 4-(R-ethynyl)phenoxy moieties (R = 4,7-di(2-thienyl)benzo[c][1,2,5]thiadiazole (**P2**), pyrene (**P3**) or pyrene-CH_2OCH_2 (**P4**)) at the four bay positions, were prepared, along with the known related derivative (R = phenyl (**P1**)), and well characterized. They have large two-photon absorption (TPA) cross-sections (σ_2), as determined by the Z-scan technique, the highest values being reached with **P2** which bears a planar π-delocalized donor moiety. **P3** is characterized by higher σ_2 values than both **P1,** as expected for the higher π-conjugation of the donor pyrene moiety with respect to phenyl, and **P4**, due to the presence of the flexible and non-conjugated CH_2OCH_2 bridge between the pyrene and the ethynyl fragment in the latter compound. The molecular geometry of **P1**-**P4** has been optimized by DFT modeling, showing that in **P2** and **P3** the bay substituents are stacked due to the π-π interactions of both pyrene and thiophene groups. The LUMO of **P1**-**P4** lyes at the same energy and is essentially delocalized on the perylene core whereas the HOMO and HOMO-1 of both **P2** and **P3** are degenerate and do not show contribution from the perylene core contrarily to that of **P1** and **P4**. The HOMO-LUMO gap is therefore essentially influenced by the HOMO which reflects the electronic charge delocalization on the bay substituents, the lower gaps being observed for **P2** and **P3**, which are characterized by the best TPA properties.

Introduction

Molecules may undergo two-photon absorption (TPA) when exposed to high-intensity light sources, reaching a final state by the simultaneous absorption of two photons, each one with half of the energy required for the electronic transition. One of the advantages of this process is the quadratic dependence with the irradiance that makes possible to confine the laser excitation in a minute spatial volume.[1-2] In addition, TPA processes allow high depth penetration and the use of low-energy photons. Thanks to these features, molecular two-photon absorption has attracted growing interest for a wide range of applications,[1-4] including 3D optical data storage[5-8] up-converted stimulated emission,[9-10] microscopy,[11-13] microfabrication,[14-15] photodynamic therapy,[16-19] localized release of bio-active species,[20] and cell imaging,[21-23] to name just a few examples. The requirements for maximizing the TPA cross-section of a chromophore include (i) long π-conjugated systems with enforced co-planarity that ensure large conjugation lengths to have high transition dipole moments, (ii) donor (D) and acceptor (A) groups at the center and ends of the molecule, and (iii) narrow one-photon and two-photon absorption bands.[2] A wide range of D and A groups have been investigated and it is generally considered that D-π-D and D-π-A-π-D structures are often more effective than A-π-A and A-π-D-π-A systems.[2] In recent years, molecular engineering directed towards TPA optimization has become very active, leading to a range of molecules of various symmetries including dipoles, quadrupoles, octupoles, and branched structures,[2, 24-31] in addition to exploring novel electronic structures such as singlet diradicaloid.[32]

Among the investigated molecules, there is a growing interest in the study of the TPA properties of perylenetetracarboxy-3,4:9,10-diimide (PTCDI) derivatives, already known for their thermal stability, chemical inertness, outstanding electrical and optical properties which led to various applications such as photoelectrochemical solar fuel generators[33-36] and luminescent devices.[37] The reason for the suitability of PTCDIs for such a large and diverse range of applications is encoded in its molecular structure: a rigid polycyclic aromatic scaffold (perylene) substituted with two dicarboxylic acid imide groups at the 3,4- and 9,10-peri-positions; the strong conjugation between the electron-rich perylene and the electron-withdrawing imide groups affords an

[a] Department of Chemistry, Università degli Studi di Milano, UdR dell'INSTM, Via Golgi 19, 20133 Milano, Italy. E-mail: alessia.colombo@unimi.it
[b] IFMRI, National Institute of Advanced Industrial Science and Technology (AIST), Ikeda, Osaka 563-8577, Japan. E-mail: k.kamada@aist.go.jp
[c] Computational Laboratory for Hybrid/Organic Photovoltaics (CLHYO), CNR-ISTM, Via Elce di Sotto 8, I-06213, Perugia, Italy. E-mail: simona@thch.unipg.it.
[d] Department of Chemistry, Materials and Chemical Engineering "Giulio Natta", Politecnico di Milano, Piazza Leonardo da Vinci 32, 20133 Milano, Italy.

Electronic Supplementary Information (ESI) available: [Tabulated TPA cross-sections values obtained with the power-scan at fix wavelength and typical Z-scan traces, NMR spectra of new compounds and Isodensity plots of the frontier molecular orbitals of P1-P4]. See DOI: 10.1039/x0xx00000x

interesting acceptor-donor-acceptor system.[38] Mendonça et al. put in evidence the interesting TPA properties of a series of PTCDI derivatives, bearing various substituents at the imide positions.[39-42] By using the open-aperture white-light continuum Z-scan technique with femtosecond laser pulses, higher TPA cross-sections σ_2 were observed for benzyl and phenylethyl substituents (*ca* 1500 GM at 654 nm) in comparison to butyl (*ca* 1000 GM), probably related to the higher planarity of the perylene moiety in these molecules.[42] When the excitation wavelength approached the linear absorption band (below 630 nm), a significant increase in σ_2 was observed, in agreement with the resonant enhancement of TPA[42] based on the four-state model with two TPA states.[43] Although the functional substitution was mostly made on the imide moieties of PTCDI in their studies,[39-42] "bay"-positions (i.e., positions 1,6,7 or 12) are also useful for structural modification of PTCDI. Such a modification at the bay positions is interesting because it can directly influence the electronic properties and geometric structure of the perylene core.[38] Marder et al. showed that a perylenetetracarboxy-3,4:9,10-diimide bearing 2,6-diisopropylphenyl groups at the imide positions and pyrrolidin-1-yl substituents in 1 and 7 bay positions has TPA cross-sections up to 2800 GM at *ca* 800 nm, close to the one-photon absorption band, along with σ_2 values up to ca 800 GM at 1000 nm.[44] Similar values were obtained by substitution of pyrrolidin-1-yl with *p*-(dibutylaminophenyl)ethynyl, whereas lower values were observed with the poorer electron donor *p*-(butoxyphenyl)ethynyl as expected for a donor-acceptor-donor structure where perylene acts as the electron-acceptor moiety.[44] Last year, Cao et al. reported that a perylenetetracarboxy-3,4:9,10-diimide bearing cyclohexyl groups at the imide positions and a π-electron-rich triphenylamine unit in 1 bay position is characterized by a σ_2 value of 130 GM at 900 nm, as determined by the Z-scan technique, a slightly higher value (140 GM) being reached by introduction of a second triphenylamine in position 7.[45] In these systems, the aromatic substituents were directly connected to the bay positions. In the same way, the TPA properties of PTCDI tetrasubstituted in the four bay positions (1,6,7,12) with directly-connected phenyl groups bearing electron donor/acceptor moieties have also been investigated. These molecules have 2,6-diisopropylphenyl groups at the imide positions and the derivative with four *p*-methoxyphenyl as bay substituents has a cross section of 180 GM at 850 nm, one order of magnitude greater respect to the reference derivative with no substituents in the bay positions.[46] It was also shown that tetrasubstitution causes twisting of the perylene core because of the steric hindrance between the phenyl rings connected at the bay positions.

Another way of bay substitution involves the use of an ether linker between the perylene core and the π-delocalized groups. For example, substitution with phenoxy groups, connected via an ether group instead of the direct connection with the aromatic ring, at the four bay positions of PTCDI bearing 2,6-diisopropylphenyl groups at the imide positions was reported. Thus, by using *p*-(sulphonic acid)phenoxy groups as bay substituents, a water soluble perylenetetracarboxy-3,4:9,10-diimide was realized with σ_2 values between 10 and 50 GM in the range 840-980 nm, as determined by the two-photon-excited fluorescence (TPEF) technique, of interest for biology applications.[47] By using the same ether-mediated bay substitution method, 2,6-diisopropylphenyl PTCDI with thiophene-based dendron substituted phenoxy groups were studied; their cross-sections are around 100-300 GM and 20-50 GM at 720 nm and 890 nm, respectively, with the TPEF technique.[48] Interestingly, the σ_2 values don't increase by increasing the number of thiophene units in the dendrons because the charge transfer character decreases in highly branched structures, due to the twisting of the perylene core which causes interruption of the charge correlation between the perylene itself and the dendrons.[48]

These interesting TPA properties of perylenetetracarboxy-3,4:9,10-diimides, bearing 2,6-diisopropylphenyl groups at the imide positions and tetrasubstituted at all bay positions *via* a flexible ether linker prompted us to prepare other members of this family (Figure 1), in order to investigate their TPA cross-sections. As substituents for the bay positions, we choose 4-(R-ethynyl)phenoxy moieties, where R is phenyl[49] (**P1**), 4,7-di(2-thienyl)benzo[c][1,2,5]thiadiazole (**P2**), pyrene (**P3**) or pyrene-CH_2OCH_2 (**P4**). Thus, the known compound **P1** could be taken as reference to measure the effect of the more π-extended structures of pyrene and di(thienyl)benzothiadiazole. Also, comparison of **P3** and **P4** would allow to study the effect of a non-conjugated linker between the lateral pyrenes and the (ethynyl)phenoxy moieties of the PTCDI core. Remarkably, the novel compound **P2** shows excellent σ_2 values (3340 ± 270 GM at 639 nm and 1530 ± 120 GM at 720 nm) much higher than those previously reported for PTCDI bearing an ether linker between the perylene core and the π-delocalized groups at the bay positions.

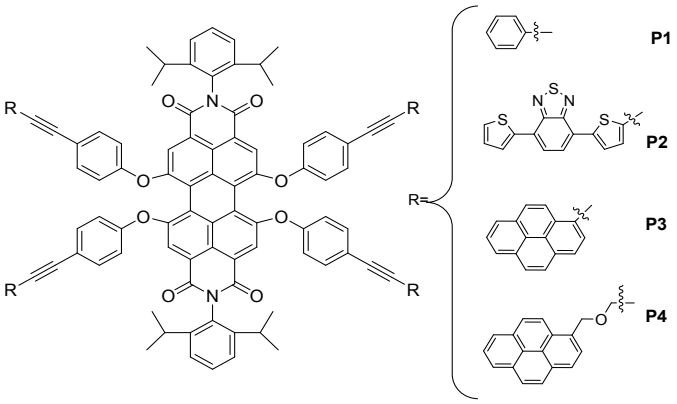

Figure 1. Structure of the investigated perylenetetracarboxy-3,4:9,10-diimide derivatives (**P1-P4**)

Results and discussion

Synthesis of perylenetetracarboxy-3,4:9,10-diimide derivatives

The known perylenetetracarboxy-3,4:9,10-diimide derivative **P1** and the related compounds **P2-P4** are readily prepared following the synthetic procedure reported in Scheme 1.

View Article Online
DOI: 10.1039/C8NJ07216F

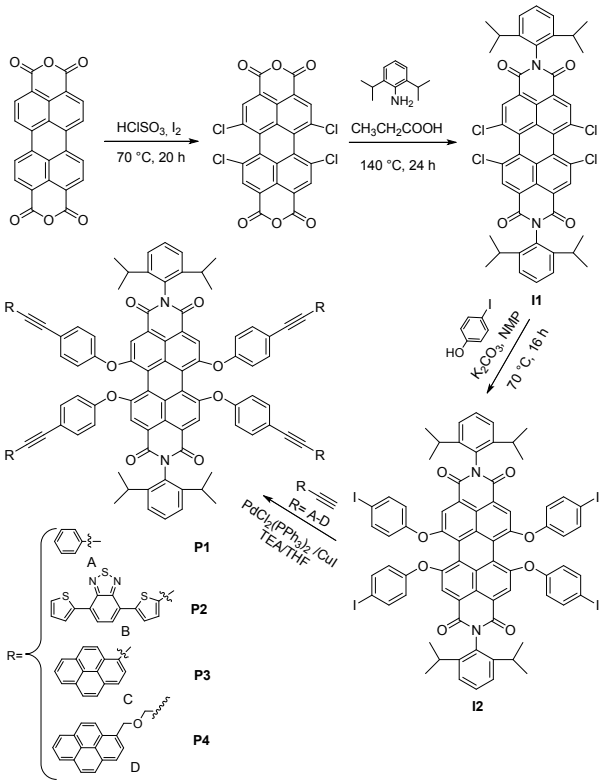

Scheme 1: Synthetic pathway of the PTCDI derivatives

The synthesis starts with the chlorination of 3,4:9,10-perylene tetracarboxylic dianhydride followed by reaction with 2,6-diisopropylaniline to give **I1.** Subsequently, the tetrakis(iodophenoxy)perylene-derivative (**I2**) is readily prepared from **I1** by reaction with *p*-iodophenol in the presence of anhydrous K_2CO_3 in 1-methyl-2-pyrrolidone (NMP). The iodo group is optimal to attach an alkynyl moiety. The four iodo substituents are easily replaced with the suitable alkyne (**A-D**), by fourfold Sonogashira coupling, affording derivatives **P1-P4** in good yields (65-80%). This reaction is carried out in THF/NEt_3 at room temperature with a $[PdCl_2(PPh_3)_2]$/CuI catalyst system (see Experimental).

One-photon absorption

The UV-Vis spectral shapes of **P1-P4** are typical of the family of perylenetetracarboxy-3,4:9,10-diimide compounds with large ε values, showing high one-photon absorption. [38, 44-46, 50-52] The parent perylenetetracarboxy-3,4:9,10-diimide bearing 2,6-diisopropylphenyl groups at the imide positions but without substituents at bay positions shows, in $CHCl_3$, an absorption band peak at 527 nm with characteristic vibronic fine structure which is attributed to the perylene core $S_0 \rightarrow S_1$ π-π* transition.[52] For the derivatives substituted with 4-(R-ethynyl)phenoxy moieties we observe a blurring of the vibronic structure and a bathochromic shift of the lowest-energy intense band, at *ca* 570-590 nm (Figure 2), as expected for the presence of tetraphenoxy bay-substituted compounds, because of the loss of rigidity due to core twisting and slight electron-donating nature of phenoxy substituents.[53,54] However, the peak position was almost the same for all substituents at bay position. In the case of **P2**, the absorption bands of the PTCDI core and the di(thienyl)benzothiadiazole moiety[55-57] are partially superimposed. At shorter wavelengths, structured bands ascribed to absorption of the aromatic moieties (pyrene, phenyl, di(thienyl)benzothiadiazole) can be noticed. It is important pointing out that the four compounds **P1-P4** are transparent at wavelengths longer than 600 nm, which makes them suitable for the investigation of two-photon absorption in the near-IR spectral range, the most interesting from an application point of view.

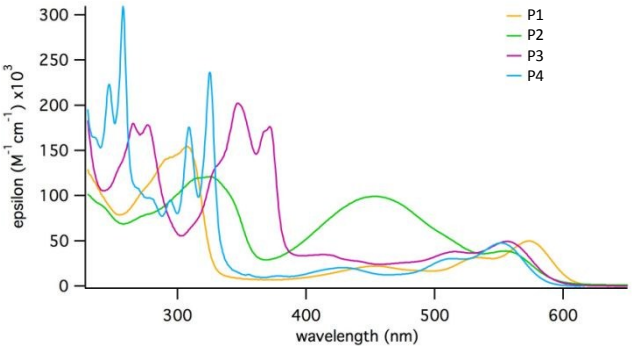

Figure 2. Absorption spectra of **P1-P4** in dichloromethane.

Two-photon absorption

Nonlinear absorption measurements were carried out on compounds **P1-P4**, dissolved in dichloromethane, by means of the Z-scan technique (see Experimental). The related two-photon absorption spectra, recorded from 638 to 800 nm, are shown in Figure 3 whereas the tabulated TPA cross-section values, obtained by confirming the incident-power dependence (power scan), are reported in the Electronic Supplementary Information (Table S1) along with the typical Z-scan traces (Figures S1-S4). The TPA properties have also been tested between 1100 and 1200 nm, but in this range of wavelengths the compounds response was under the detection limit of 3 GM.

The TPA spectra of the four compounds (Figure 3) show a similar feature to each other: the maximum σ_2 value is at the investigated shortest wavelength (639 nm), close to the one-photon absorption (OPA) band. At longer wavelengths, the σ_2 intensity decreases with a shoulder (**P2**, **P3**) or small peak (**P1**, **P4**) at 720 nm.

The TPA magnitude differs considerably depending on the substituents at bay positions.

P2 shows the highest σ_2 values (3340 ± 270 GM at 639 nm and 1530 ± 120 GM at 720 nm, Table S1) thanks to the π-delocalized electron-donor di(thienyl)benzothiadiazole moieties that contribute to the planarity of the branches, as confirmed by DFT modelling (see later).

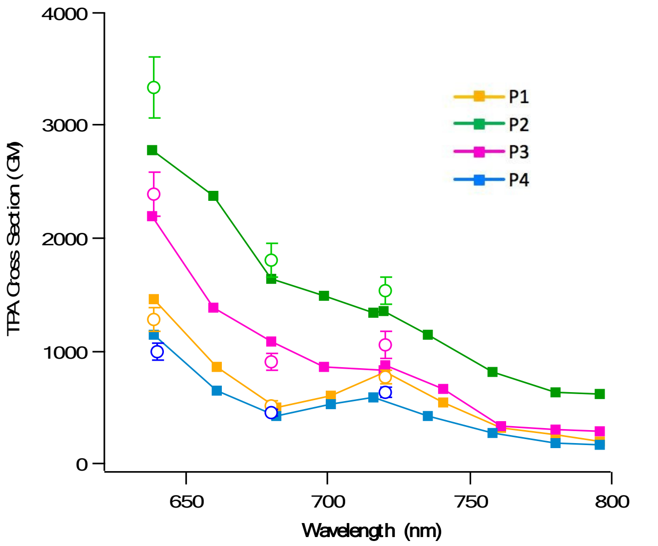

Figure 3. TPA spectra of PTCDI derivatives: the full markers are the values obtained with the wavelength scan at a fix power, while the empty markers with error bars are the ones obtained with the power scan at a fixed wavelength.

P3 has lower but still high σ$_2$ values (2390 ± 200 GM at 639 nm and 1060 ± 120 GM at 720 nm, Table S1) thanks to the planar pyrene substituents. **P1** has the same π-conjugated backbone as **P3** but bears phenyl instead of the more π-delocalized pyrene, which is the cause of its lower σ$_2$ values (1280 ± 100 GM at 639 nm and 770 ± 60 GM at 720 nm, Table S1). **P3** can be discussed in comparison to **P4** since both of these compounds possess pyrene moieties. While in the former the pyrene is linked directly to the alkyne, in the latter the conjugation path is interrupted by a dimethylenether bridge. This bridge not only breaks the π-conjugation of the branches, but also reduce their planarity. As a consequence, the σ$_2$ values for **P4** (1000 ± 80 GM at 639 nm and 630 ± 50 GM at 720 nm, Table S1) are lower than for the parent **P3**, which has better π-conjugated branches.

The monotonic increase of the TPA values at shorter wavelengths (*ca* 640 nm), which gave the maximum value of each compound, is caused by the resonance enhancement of TPA through decreasing detuning energy of the one-photon absorption transition[43] like other reported PTCDIs.[42,44] Observing the spectra, the spectral shape in the resonance enhancement region at the shorter wavelength is almost the same and it isn't much influenced by the nature of the investigated substituents at the bay positions. This is consistent with the lowest energy one-photon absorption peaks of **P1**-**P4** (Figure 1) being at wavelengths close to each other. On the other hand, the substituents influence the σ$_2$ magnitude in the resonance enhanced region and a better π-conjugated substituent gives a larger magnitude. These results suggest that the inherent transition probability of TPA is enhanced by the bay substituent with better π-conjugation because the magnitude of the TPA spectral is defined by the transition dipole moments products (in the numerator in the theoretical expression of σ$_2$) while its spectral shape is defined by the frequency term (in the denominator) in which the detuning energy is involved. [43]

In addition to the σ$_2$ magnitude in the resonance enhancement part, the substituents influence the shape and intensity of the shoulder at lower wavelength. This shows that the transition probability of TPA is higher for the compound depending on the π-conjugation of the bay substituent. The TPA transition probability is proportional to the product of the transition dipole moment, $|\mu_{fi}|^2$ $|\mu_{ig}|^2$, where f,i,g means the final, intermediate, and ground states, respectively. Clearly the final state is higher than S_1 for the shoulder band and the TPA transition related to the resonance enhancement from their transition energies. On the other hand, S_1 (i=1) is the most probable candidate for the intermediate state because it is the excited state closest to the incident photon energy. Moreover, the lowest-energy one-photon absorption peak is insensitive to the bay substituents (Figure 1), showing that the bay substitution does not perturb the S_1, which is supported by the confined MO in the perylene core. Thus, the bay substitution has no influence on μ_{1g} but largely affects μ_{f1}, resulting in the change of σ$_2$ by the bay substitution. Namely, the TPA properties are governed by the properties of the excited states. This type of behaviour, i.e. the one-photon absorption is insensitive but the TPA magnitude is sensitive to the substituents, was observed for systems where rotation of the π-extension arms was restricted to the π-core.[58]

Remarkably, the σ$_2$ values of **P1-P4** are quite high (in the range 630-1530 GM) even at 720 nm where the one-photon absorption resonance enhancement is negligible, putting in evidence the goodness of 4-(R-ethynyl)phenoxy groups as substituents for the four bay positions in order to design highly TPA-active PTCDI derivatives. The use of an adequate π-conjugated donor R fragment may allow optimization of the σ$_2$ values.

DFT Modeling

The molecular geometry of **P1**-**P4** has been optimized in CH_2Cl_2 solution and the optimized molecular structures are shown in Figure 4.

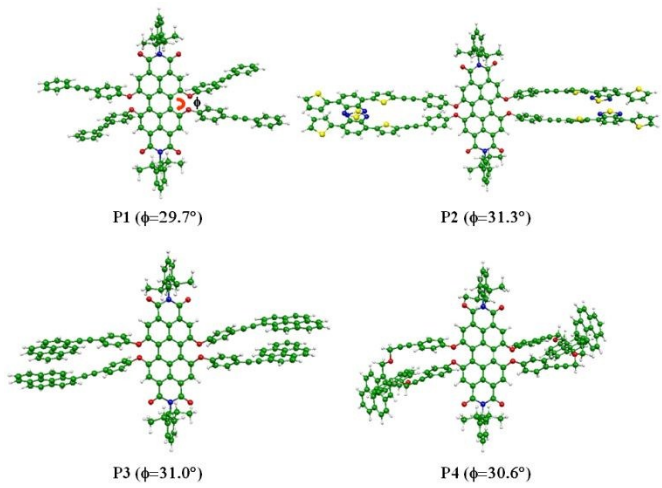

Figure 4. Optimized molecular structure of the investigated compounds **P1-P4** together with the dihedral angle ϕ which measures the twisting torsion of the perylene core.

We found that the perilene core of the four compounds is not planar and the dihedral angle (ϕ) which measures the twisting torsion of the perylene core due to the bay substituents has been computed in between 29.7°- 31.7° (see Figure 4). It is interesting to notice that in **P2** and **P3**, which are characterized by the best TPA properties, the bay substituents are stacked due to the π-π interactions of both pyrene and thiophene groups. This geometrical

constraint is not present in **P1**, while in **P4** the outer pyrenes are prevented to be stacked and orient each other almost in a perpendicular configuration due to CH-π interactions between the pyrene hydrogen and the conjugated π system of the other pyrene. The twisting torsion seems to be only marginally affected by the substituents (the maximum variation being computed 2°), nevertheless the larger dihedral ϕ angles are computed for **P2** and **P3**.

Besides, we compared the frontier molecular orbitals of **P1-P4** to analyze the relative energy alignment and the electronic charge distribution; in Figure 5 we report the energy levels of the highest occupied molecular orbitals (HOMOs) and of the lowest unoccupied molecular orbitals (LUMOs) together with the isodensity plots of HOMO/LUMO of all investigated compounds. In addition the isodensity plots of HOMO-1 and LUMO+1 of **P1-P4** are collected in the Electronic Supplementary Information. The HOMO of **P1** is the result of a combination of p orbitals of the central perylene carbons and of the carbons of the two opposite bay substituents plus the p orbitals of the four oxygen atoms which act as linkers between the substituents and the perylene core. The HOMO-1/HOMO-4 in a range of 0.2 eV are different p orbitals combinations on the carbons and oxygens of the bay substituents, with no contribution from the perylene. The HOMO and HOMO-1 of both **P2** and **P3** are degenerate and does not show contribution from the perylene core. In **P2** both HOMO and HOMO-1 are the mixing of p orbitals of the carbon atoms of all the four chains with different coefficients, while in **P3** they are mainly delocalized on the triple CC bond and pyrene groups of the four bay substituents . Both the HOMOs of **P2** and **P3** are stabilized by ca. 0.5 eV with respect to the **P1** HOMO. The HOMO and HOMO-1 of **P4** are degenerate and are delocalized on the two opposite pyrene groups in the same orientation, while at lower energy by 0.17 eV, the degenerate couple HOMO-2/HOMO-3 lyes showing an electronic charge distribution on the two pyrene groups with a different orientation. The LUMO of compounds **P1-P4** lyes at the same energy and is essentially delocalized on the same molecule region: the perylene core. The HOMO-LUMO gap is therefore essentially influenced by the HOMO which reflects the electronic charge delocalization on the bay substituents. The HOMO-LUMO gap of **P2** and **P3** are similar and the increasing order is **P2**<**P3**<**P4**<**P1**.

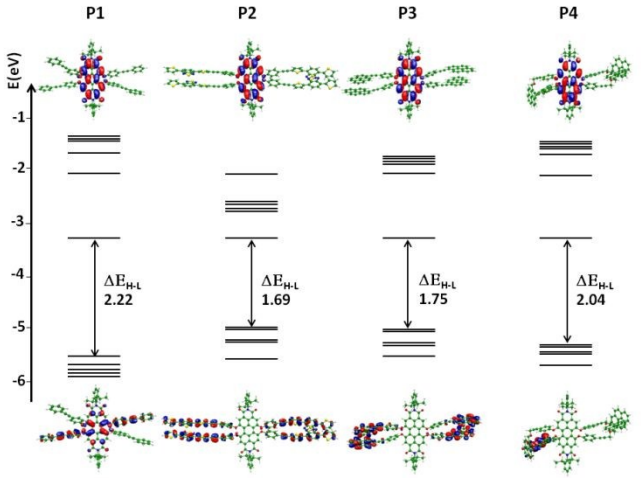

Figure 4. Schematic diagram of the energy levels of **P1-P4** compounds. Surface isodensity plots (isodensity contour: 0.02) of HOMO (bottom) and LUMO (up) are also shown.

Experimental

View Article Online
DOI: 10.1039/C8NJ03216E

Synthesis of perylenetetracarboxy-3,4:9,10-diimide derivatives

Reagents and alkyne derivatives (A-C). All reagents, including phenylacetylene **A**, were obtained from commercial sources and used without further purification. 1-Ethynylpyrene (**C**) was readily prepared, as previously reported,[59] from 1-bromopyrene by Sonogashira coupling reaction with trimethylsilyl acetylene followed by TMS removal in the presence of tetrabutylammonium fluoride. The same synthetic pathway was used to obtain alkyne **B**.[56]

N,N'-bis(2,6-diisopropylphenyl)-1,6,7,12-tetrachloro-3,4:9,10-perylenetetracarboxydiimide (**I1**) was prepared as reported in Scheme **1** following a well-known synthetic procedure.[53, 60, 61]

Synthesis of the alkyne D. First, the 1-hydroxymethyl pyrene intermediate was prepared as follows: to a solution of 1-pyrenecarboxaldehyde (1.0 g, 4.34 mmol) in dry MeOH/CH_2Cl_2 (1/1, 17 mL), under argon atmosphere at 0°C, was added $NaBH_4$ (181.2 mg, 4.8 mmol) in three portions; the reaction mixture was stirred at 0°C for 30 min and at room temperature for 1 h; the mixture was diluted with water (50 mL) and extracted with CH_2Cl_2 (3x50mL); the organic layer was dried on Na_2SO_4 and the solvent was removed at reduced pressure to give the solid product (yield = 97 %).

^{1}H-NMR (400 MHz; $CDCl_3$) δ ppm: 5.44 (2H, s), 8.02-8.11 (4H, m), 8.17-8.24 (4H, m), 8.41 (1H, d, J = 9.21 Hz).

1-((2-propynyloxy)methyl)pyrene (**D**) was then prepared as follows: 1-hydroxymethyl pyrene (601 mg, 2.6 mmol) was added under argon to a solution at 0°C of NaH (68.6mg, 2.86 mmol) in dry DMF (10.4 mL); the reaction mixture was stirred at 0°C for 10 min and then at room temperature for 1 h; propargyl chloride (206 µL, 2.86 mmol) was added at 0°C and the mixture was stirred at room temperature overnight; the reaction mixture was quenched with water (50 mL) and extracted with ethylacetate (3x50mL); the organic layer was dried on Na_2SO_4 and the solvent was removed at reduced pressure to give the crude product that was purified by flash chromatography using hexane/dichloromethane 1/1 as eluent; the pure product was obtained in 90% yield.

^{1}H-NMR (400 MHz; $CDCl_3$) δ ppm: 2.61 (1H, t, *J* = 2.36 Hz), 4.32 (2H, d, *J* = 2.36 Hz), 5.35 (2H, s), 8.02-8.10 (4H, m), 8.16-8.23 (4H, m), 8.43 (1H, d, *J* = 9.22 Hz). Anal. Calcd.(%) for $C_{20}H_{14}O$: C, 88.86; H, 5.22. Found: C 88.90; H 5.23.

Synthesis of 1,6,7,12-tetrakis(4-iodophenoxy)-N,N'-(2,6-diisopropylphenyl)perylenetetracarboxy-3,4:9,10-diimide (I2). In a 100 mL flask, under nitrogen atmosphere, a solution of tetrachloroperylene-tetracarboxdiimide **I1** (400 mg, 0.46 mmol) 4-iodophenol (616 mg, 2.8 mmol) and anhydrous K_2CO_3 (193.4 mg, 1.4 mmol) in 1-methyl-2-pyrrolidone (23 mL) was stirred overnight at 70 °C. The reaction mixture was cooled to room temperature and poured into 2N HCl (64 mL). The product was extracted with ethylacetate (100mL) and the organic phase washed three times with water (100 mL), and dried over Na_2SO_4. The crude product was purified by flash chromatography (eluent: Hexane: CH_2Cl_2 1:4) to give **I2** as red solid in 80% yield.

^{1}H-NMR (400 MHz; $CDCl_3$) δ ppm: 8.26 (4H, s), 7.61 (2H, d, *J* = 8.74 Hz), 7.47 (16 H, t, *J* = 7.68 Hz), 7.30 (4H, t, *J* = 7.76 Hz), 2.70 (4H, m), 1.14-1.24 (24H, m). MS(FAB$^+$): *m/z* 1585 (calc. 1584.0)

General procedure for the syntheses of compounds P1-P4. Compound **I2** (300 mg, 0.19 mmol) was dissolved in a degassed mixture of triethylamine (50 mL) and dry THF (14 mL) under argon. Then $[PdCl_2(PPh_3)_2]$ (21.1 mg, 0.03 mmol), CuI (11.42 mg, 0.06 mol), PPh_3 (15.7 mg, 0.06 mmol) and the suitable alkyne **A-D** (1.14 mmol) were added. The reaction mixture was stirred at 70°C overnight, and then the solvent was removed under reduced pressure. The crude product was purified by column chromatography on silica gel.

1,6,7,12-Tetrakis[4-(phenylethynyl)phenoxy-N,N'-(2,6-diisopropylphenyl)perylenetetracarboxy-3,4:9,10-diimide (P1) was prepared following the above reported general procedure using 160 µL (d=0.95g/mL) of phenylacetylene (**A**), the eluent for flash chromatography being hexane/dichloromethane 1/1. The pure product was obtained as dark solid in 70% yield.

^{1}H-NMR (400 MHz; $CDCl_3$) δ ppm: 8.32 (4H, s), 7.54-7.49 (20H, m), 7.36-7.30 (14 H, m), 6.96 (8H, d, *J* = 8.76 Hz), 2.71 (4H, m), 1.18-1.15 (24H, m). MS(FAB$^+$): *m/z* 1481 (calc. 1479.5). Anal. Calcd.(%) for $C_{104}H_{74}N_2O_8$: C 84.42, H 5.04, N 1.89. Found: C 84.46, H 5.03, N 1.90.

1,6,7,12-Tetrakis[4-(4-(5-ethynylthiophen-2-yl)-7-(thiophen-2-yl)benzo[c][1,2,5]thiadiazole) phenoxy-N,N'-(2,6-diisopropylphenyl)perylenetetracarboxy-3,4:9,10-diimide (P2) was prepared starting from 369 mg of alkyne **B** , the eluent for flash chromatography being hexane/dichloromethane 1/1 and then hexane/dichloromethane 1/5. The pure product was obtained as dark red solid in 65% yield. ^{1}H-NMR (400 MHz; $CDCl_3$) δ ppm: 8.39 (4H, s), 8.10 (4H, dd, *J* =3.7 Hz, *J* =1.0 Hz), 7.98 (4H, d, *J* = 3.7 Hz), 7.91 (4H, d, *J* = 7.6 Hz), 7.88 (4H, d, *J* = 7.6 Hz), 7.51-7.45 (16H, m) 7.36-7.31(6H, m), 7.24 (4H, dd, *J* =1.0 Hz, *J* =3.7 Hz), 6.86 (8H, d, *J* = 8.6 Hz), 2.75 (4H, m), 1.19-1.17 (24H, m). ^{13}C-NMR (100 MHz; CD_2Cl_2) δ ppm: 145.85, 133.56, 129.44, 128.28, 127.08, 126.19, 125.54, 124.46, 119.98, 94.62, 29.68,29.13, 23.72. MS(FAB$^+$): *m/z* 2369 (calc. 2368.9). Anal. Calcd.(%) for $C_{136}H_{82}N_{10}O_8S_{12}$: C 68.95, H 3.49, N 5.91. Found: C 68.99, H3.53, N 5.92. Emission λ_{max} = 602 nm (toluene); fluorescence quantum yield = 0.05.

1,6,7,12-Tetrakis[4-(pyrenethynyl)phenoxy-N,N'-(2,6-diisopropylphenyl)perylenetetracarboxy-3,4:9,10-diimide (P3) was prepared starting from 258 mg of alkyne **C**, the eluent for flash chromatography being hexane/dichloromethane 1/1 and then hexane/dichloromethane 3/7. The pure product was obtained in 80% yield. ^{1}H-NMR (400 MHz; $CDCl_3$) δ ppm: 8.63 (4H, d, *J* = 9.2 Hz), 8.46 (4H, s), 8.16 (12H, d, *J* = 8.4 Hz), 8.06-7.94 (20H, m), 7.73 (8H, d, *J* = 8.8 Hz), 7.34 (4H, d, *J* = 7.6 Hz), 7.13 (8H, d, *J* = 8.4 Hz), 2.83-2.76 (4H, m), 1.20 (24H, d, *J* = 6.8 Hz). ^{13}C-NMR (100 MHz; CD_2Cl_2) δ ppm: 145.85, 133.56, 129.44, 128.28, 127.08, 126.19, 125.54, 124.46, 119.98, 94.62, 29.68,29.13, 23.72. MS(FAB$^+$): *m/z* 1978. (calc. 1976.7) Anal. Calcd.(%) for $C_{144}H_{90}N_2O_8$: C 87.52, H 4.59, N 1.42. Found: C 87.68, H 4.60, N 1.43. Emission λ_{max} = 602 nm (toluene); fluorescence quantum yield = 0.03.

1,6,7,12-Tetrakis[4-(1-((2-propynyloxy)methyl)pyrene)phenoxy-N,N'-(2,6-diisopropylphenyl)perylenetetracarboxy-3,4:9,10-diimide (P4) was prepared starting from 308 mg of alkyne **D**, the eluent for flash chromatography being hexane/dichloromethane 1/1 and then ethylacetate/dichloromethane 25/1. The pure product was obtained in 77% yield. ^{1}H-NMR (400 MHz; CD_2Cl_2) δ ppm: 8.44-8.41 (4H, d, *J* = 9.2 Hz), 8.33 (4H, s), 8.23-8.20 (8H, m), 8.16-8.12 (8H, m), 8.09-8.00 (16H, m), 7.52-7.50 (10H, m), 7.35 (4H, d, *J* = 8 Hz), 7.02 (8H, d, *J* = 8.8 Hz), 5.35 (8H, s), 4.47 (8H, s), 2.79-2.71 (4H, m), 1.16 (24H, d, *J* = 6.8 Hz). ^{13}C-NMR (100 MHz; CD_2Cl_2) δ ppm: 163.07, 155.61, 155.29, 145.94, 133.65, 131.40, 131.17, 130.84, 130.75, 129.53, 127.65, 127.46, 127.42, 127.30, 125.97, 125.24, 125.21, 124.44, 124.05, 123.46, 123.23, 120.94, 119.68, 119.01, 85.55, 70.01, 57.98, 29.09, 23.68. MS(FAB$^+$): *m/z* 2153 (calc. 2152.5) Anal. Calcd.(%) for $C_{152}H_{106}N_2O_{12}$: C 84.82, H 4.96, N 1.30. Found: C 84.86, H 4.98, N 1.30. Emission λ_{max} = 602 nm (toluene); fluorescence quantum yield = 0.40.

One-photon absorption.

The UV-Vis spectra of the samples solution in dichloromethane were recorded by a *Shimadzu UV-3150* spectrometer using quartz cells.

Photoluminescence

Photoluminescence quantum yields were measured using a C11347 Quantaurus – QY Absolute Photoluminescence Quantum Yield Spectrometer (Hamamatsu Photonics K.K), with a 150 W Xenon lamp, an integrating sphere and a multichannel detector, in a toluene solution.

Two-photon absorption activity measurements.

All open-aperture Z-scan measurements[62] were performed at AIST in Osaka. The setup for the Z-scan measurements were reported elsewhere.[63] A femtosecond, wavelength-tunable laser (optical parametric amplifier, SpectraPhysics TOPAS Prime) was employed as light source to obtain the spectrum. Typical pulsewidth was 120 fs and the repetition rate was 1 kHz. First, the outline of the TPA spectrum was measured at a single excitation power (0.4 mW, corresponding to the on-axis optical intensity at the focal point of 99-150 GW/cm^2) by assuming that the observed open-aperture Z-scan signal originates from the TPA process (filled dots in Figure 3). Then the assumption was confirmed and the precise value of the TPA cross-sections (σ_2) were obtained by changing the excitation power (open dots with experimental errors in Figure 3). Finally, the relative TPA spectrum (filled dots) was superimposed on the absolute TPA spectrum (open dots). For all measurements, a in-house standard compound (MPPBT in DMSO)[64] was measured under the same conditions and used for the spectral correction of σ_2.

DFT Calculations

All the calculations were performed with Gaussian09 (G09),[65] without any symmetry constraints. The molecular geometry of all compounds has been optimized by a Density Functional theory (DFT) approach using a 6-31G* basis set[66] the B3LYP[67] exchange-correlation functional integrated with the D3-BJ moldel to include the dispersion interactions.[68] We optimized the geometries in CH_2Cl_2 solution including solvation effects by means of the conductor-like polarizable continuum model (C-PCM)[69-70] as implemented in G09.

Conclusions

In summary we prepared and well characterized

perylenetetracarboxy-3,4:9,10-diimides, bearing 2,6-diisopropylphenyl groups at the imide positions. Three of them have highly π-delocalized 4-(R-ethynyl)phenoxy moieties (R = phenyl (**P1**), 4,7-di(2-thienyl)benzo[c][1,2,5]thiadiazole (**P2**) or pyrene (**P3**)) at the four bay positions whereas one (R = pyrene-CH_2OCH_2 (**P4**)) has poor delocalization due to the presence of the non-conjugated CH_2OCH_2 moiety. They have high TPA cross-sections, as determined by the Z-scan technique, similar to that obtained for PTCDIs bearing pyrrolidin-1-yl substituents in 1 and 7 bay positions[44] and much higher than that previously reported for PTCDIs having an ether linker between the perylene core and the π-delocalized groups.[47,48] While approaching the one-photon absorption band, at *ca* 640 nm, there is a monotonic increase of the TPA values caused by the resonance enhancement of nonlinearity via the one-photon resonance process. At longer wavelength (720 nm), the σ_2 values of **P1-P4** are still quite high (in the range 630-1530 GM), putting in evidence the goodness of 4-(R-ethynyl)phenoxy groups as substituents for the bay positions in order to design highly TPA-active PTCDI derivatives. Besides, remarkably, the bay substituent strongly affects the σ_2 magnitude while it does not influence the one-photon absorption peak to S_1 excited state. These facts suggest that the influence of the bay substitution is mainly caused by the higher excited state which is the final state of the TPA transition (S_f) through the transition dipole moment between the excited states μ_{f1} (i.e. of the transition of $S_1 \rightarrow S_f$).

It turned out that **P2** shows the highest σ_2 values thanks to the di(thienyl)benzothiadiazole moieties that contribute to the planarity of the π-delocalized branches. **P3** is characterized by higher σ_2 values than both **P1**, as expected for the higher π-conjugation of the donor pyrene moiety with respect to phenyl, and **P4**, due to the presence of the flexible and non-conjugated CH_2OCH_2 bridge between the pyrene and the ethynyl fragment in the latter. This bridge not only breaks the π-conjugation in the four branches, but also reduce their planarity, preventing the stacking of the outer pyrenes. Remarkably, in **P2** and **P3,** the most TPA active compounds, the bay substituents are stacked due to the π-π interactions of pyrene and thiophene groups, respectively. The LUMO of **P1-P4** lyes at the same energy and is essentially delocalized on the perylene core whereas the HOMO and HOMO-1 of both **P2** and **P3** are degenerate and do not show contribution from the perylene core contrarily to that of **P1** and **P4**. The HOMO-LUMO gap is therefore essentially influenced by the HOMO which reflects the electronic charge delocalization on the bay substituents, the lower gaps being observed for **P2** and **P3**, which are characterized by the best TPA properties.

These results clearly show that, in this kind of PTCDI derivatives, the use of an adequate π-conjugated donor R fragment allows optimization of the σ_2 values. Functionalising the perylene core at the bay positions offers a high synthetic flexibility and a big choice of substituents and π-conjugated patterns that will surely lead to novel TPA-active PTCDI compounds for various applications in the near future.

Acknowledgements

This work was supported by MIUR and CNR, in Italy, and by a Grant-in-Aid for Scientific Research on Innovative Areas "Photosynergetics" (No. JP26107004, K.K.) from MEXT and a Grant-in-Aid for Scientific Research (No. JP25248007, K.K.) from JSPS, Japan. We deeply thank Dr Stefania Righetto and Dr Daniele Marinotto for photoluminescence measurements.

References

1 G. S. He, L. S. Tan, Q. Zheng and P. N. Prasad, *Chem. Rev.,* 2008, **108**, 1245.
2 M. Pawlicki, H. A. Collins, R. G. Denning and H. L. Anderson, *Angew. Chem. Int. Ed.*, 2009, **48**, 3244.
3 Q. Zhang, X. Tian, H. Zhou, J. Wu and Y. Tian, *Materials*, 2017, **10**, 223, 1.
4 H. M. Kim and B. R. Cho, *Chem. Rev.,* 2015, **115**, 5014.
5 S. Kawata and Y. Kawata, *Chem. Rev.,* 2000, **100**, 1777.
6 A. S. Dvornikov, E. P. Walker and P. M. Rentzepis, *J. Phys. Chem. A*, 2009, **113**, 13633.
7 J. Yu, Y. Cui, C. D. Wu, Y. Yang, B. Chen and G. Qian, *J. Am. Chem. Soc.*, 2015, **137**, 4026.
8 K. Kamada, K. Satoh, Y. Tanaka, *Jpn. J. Appl. Phys.* 2016, **55,** 09SB04.
9 G. S. He, H. Y. Qin, Q. Zheng, P. N. Prasad, S. Jockusch, N. J. Turro, M. Halim, D. Sames, H. Agren and S. He, *Phys. Rev. A: At., Mol., Opt. Phys.,* 2008, **77**, 10.
10 J. J. Jasieniak, I. Fortunati, S. Gardin, R. Signorini, R. Bozio, A. Martucci and P. Mulvaney, *Adv. Mater.,* 2008, **20**, 69.
11 W. R. Zipfel, R. M. Williams and W. W. Webb, *Nat. Biotechnol.,* 2003, **21**, 1368.
12 A. Picot, A. D'Aleo, P. L. Baldeck, A. Grichine, A. Duperray, C. Andraud and O. Maury, *J. Am. Chem. Soc.,* 2008, **130**, 1532.
13 Y. I. Park, K. T. Lee, Y. D. Suh and T. Hyeon, *Chem. Soc. Rev.*, 2015, **44**, 1302.
14 K. D. Belfield, K. J. Schafer, Y. U. Liu, J. Liu, X. B. Ren and E. W. Van Stryland, *J. Phys. Org. Chem.,* 2000, **13**, 837.
15 C. N. LaFratta, J. T. Fourkas, T. Baldacchini and R. A. Farrer, *Angew. Chem. Int. Ed.*, 2007, **46**, 6238.
16 W. G. Fisher, W. P. Partridge Jr., C. Dees and E. A. Wachter, *Photochem. Photobiol.,* 1997, **66**, 141.
17 J. Arnbjerg, M. Johnsen, P. K. Frederiksen, S. E. Braslavsky and P. R. Ogilby, *J. Phys. Chem. A,* 2006, **110**, 7375.
18 L. Beverina, M. Crippa, M. Landenna, R. Ruffo, P. Salice, F. Silvestri, S. Versari, A. Villa, L. Ciaffoni, E. Collini, C. Ferrante, S. Bradamante, C. M. Mari, R. Bozio and G. A. Pagani, *J. Am. Chem. Soc.,* 2008, **130**, 1894.
19 G. Chen, I. Roy, C. Yang and P. N. Prasad, *Chem. Rev.*, 2016, **116**, 2826.
20 G. C. R. Ellis-Davies, *Nat. Methods,* 2007, **4**, 619.
21 E. Baggaley, S. W. Botchway, J. W. Haycock, H. Morris, I. V. Sazanovich, J. A. G. Williams and J. A. Weinstein, *Chem. Sci*., 2014, **5**, 879 and references therein.
22 E. Baggaley, J. A. Weinstein and J. A. G. Williams, *Coord. Chem. Rev.,* 2012, **256**, 1762 and references therein.
23 J. Li, F. Cheng, H. Huang, L. Li and J. J. Zhu, *Chem. Soc. Rev.*, 2015, **44**, 7855.
24 L. Porrès, C. Katan, O. Mongin, T. Pons, J. Mertz, M. Blanchard-Desce, *J. Mol. Struct.,* 2004, **704**, 17.
25 S. Righetto, S. Rondena, D. Locatelli, D. Roberto, F. Tessore, R. Ugo, S. Quici, S. Roma, D. Korystov and V. I. Srdanov, *J. Mater. Chem.,* 2006, **16**, 1439 and references therein.
26 S. Mazzucato, I. Fortunati, S. Scolaro, M. Zerbetto, C. Ferrante, R. Signorini, D. Pedron, R. Bozio, D. Locatelli, S. Righetto, D. Roberto, R. Ugo, A. Abbotto, G. Archetti, L. Beverina and S. Ghezzi, *Phys. Chem. Chem. Phys.*, 2007, **9,** 2999.
27 L. Grisanti, C. Sissa, F. Terenziani, A. Painelli, D. Roberto, F. Tessore, R. Ugo, S. Quici, I. Fortunati, E. Garbin, C. Ferrante and R. Bozio, *Phys. Chem. Chem. Phys.*, 2009, **11**, 9450.
28 C. Dragonetti, M. Balordi, A. Colombo, D. Roberto, R. Ugo, I.

Fortunati, E. Garbin, C. Ferrante, R. Bozio, A. Abbotto and H. Le Bozec, *Chem. Phys. Lett.*, 2009, **475**, 245.
29 F. Todescato, I. Fortunati, S. Carlotto, C. Ferrante, L. Grisanti, C. Sissa, A. Painelli, A. Colombo, C. Dragonetti and D. Roberto, *Phys. Chem. Chem. Phys.*, 2011, **13**, 11099.
30 A. Colombo, C. Dragonetti, D. Roberto, A. Valore, C. Ferrante, I. Fortunati, A. Lorena Picone, F. Todescato and J. A. G. Williams, *Dalton Trans*., 2015, **44**, 15712.
31 A. Colombo, E. Garoni, C. Dragonetti, S. Righetto, D. Roberto, N. Baggi, M. Escadeillas, V. Guerchais and K. Kamada, Polyhedron, 2018, **140**, 116.
32 K. Kamada, K. Ohta, T. Kubo, A. Shimizu, Y. Morita, K. Nakasuji, R. Kishi, S. Ohta, S. Furukawa, H. Takahashi, M. Nakano, *Angew. Chem. Int. Ed.* 2007, **46,** 354; K. Kamada, K. Ohta, A. Shimizu, T. Kubo, R. Kishi, H. Takahashi, E. Botek, B. Champagne, M. Nakano, *J. Phys. Chem. Lett.* 2010, **1**, 937; K. Kamada, S. Fuku-en, S. Minamide, K. Ohta, R. Kishi, M. Nakano, H. Matsuzaki, H. Okamoto, H. Higashikawa, K. Inoue, S. Kojima, Y. Yamamoto, *J. Am. Chem. Soc.* 2013, **135,** 232.
33 F. Ronconi, Z. Syrgiannis, A. Bonasera, M. Prato, R. Argazzi, S. Caramori, V. Cristino and C. A. Bignozzi, *J. Am. Chem. Soc.,* 2015*,* **137**, 4630.
34 S. Berardi, V. Cristino, M. Canton, R. Boaretto, R. Argazzi, E. Benazzi, L. Ganzer, R. Borrego Varillas, G. Cerullo, Z. Syrgiannis, F. Rigodanza, M. Prato, C. A. Bignozzi and S. Caramori, *J. Phys. Chem.,* 2017, **121**, 17737.
35 G. Griffini, M. Levi and S. Turri, *Renewable Energy*, 2015, **78**, 288.
36 G. Griffini, L. Brambilla, M. Levi, M. Del Zoppo and S. Turri, *Sol. Energy Mater. Sol. Cells*, 2013, **111**, 41.
37 E. Kozma, W. Mróz, F. Villafiorita-Monteleone, F. Galeotti, A. Andicsová-Eckstein, M. Catellani and C. Botta, *RSC Adv.*, 2016, **6**, 61175.
38 F. Würthner, C.R. Saha-Möller, B. Fimmel, S. Ogi, P. Leowanawat, and D. Schmidt, *Chem. Rev.* 2016, **116**, 962.
39 L. De Boni, C. J. L. Constantino, L. Misoguti, R. F. Aroca, S. C. Zilio and C. R. Mendonça, *Chem. Phys. Lett.,* 2003, **371**, 744.
40 S. L. Oliveira, D. S. Corrêa, L. Misoguti, C. J. L. Constantino, R. F. Aroca, S. C. Zilio and C. R. Mendonça, *Adv. Mater.,* 2005, **17**, 1890.
41 D. S. Correa, S. L. Oliveira, L. Misoguti, S. C. Zilio, R. F. Aroca, C. J. L. Constantino and C. R. Mendonça, *J. Phys. Chem. A,* 2006, **110**, 6433.
42 E. Piovesan, D. L. Silva, L. De Boni, F. E. G. Guimaraes, L. Misoguti, R. Zalesny, W. Bartowiak and C. R. Mendonça, *Chem. Phys. Lett*., 2009, **479**, 52.
43 K. Kamada, K. Ohta, Y. Iwase, K. Kondo, *Chem. Phys. Lett.* 2003, **372,** 386.
44 Z. An, S. A. Odom, R. F. Kelley, C. Huang, X. Zhang, S. Barlow, L. A. Padilha, J. Fu, S. Webster, D. J. Hagan, E. W. Van Stryland, M. R. Wasielewski and S. R. Marder, *J. Phys. Chem. A,* 2009, **113**, 5585.
45 L. Cao, L. Xu, D. Zhang, Y. Zhou, Y. Zheng, Q. Fu, X.-F. Jiang and F. Lu, *Chem. Phys. Lett.,* 2017, **682**, 133.
46 B. Pagoaga, O. Mongin, M. Caselli, D. Vanossi, F. Momicchioli, M. Blanchard-Desce, G. Lemercier, N. Hoffmann and G. Ponterini, *Phys. Chem. Chem. Phys.* 2016, **18**, 4924.
47 A. Margineanu, J. Hofkens, M. Cotlet, S. Habuchi, A. Stefan, J. Qu, C. Kohl, K. Müllen, J. Vercammen, Y. Engelborghs, T. Gensch and F. C. De Schryver, *J. Phys. Chem. B*, 2004, **108**, 12242.
48 J. Zhang, M. K. R. Fischer, P. Bäuerle and T. Goodson III, *J. Phys. Chem. B*, 2013, **117**, 4204.
49 C. Flors, I. Oesterling, T. Schnitzler, E. Fron, G. Schweitzer, M. Sliwa, A. Herrmann, M. van der Auweraer, F. C. de Schryver, K. Mu1llen and J. Hofkens, *J. Phys. Chem.,* 2007, *111*, 4861.
50 M. Adachi, Y. Murata and S. Nakamura, *J. Phys. Chem.*, 1995, **99**, 14240.
51 S. K. Lee, Y. Zu, A. Herrmann, Y. Geerts, K. Mullen and A. J. Bard, *J. Am. Chem. Soc*., 1999, **121**, 3513.
52 C.-C. Chao, M.-k. Leung, Y. O. Su, K.-Y. Chiu, T.-H. Lin, S.-J. Shieh and S.-C. Lin, *J. Org. Chem.,* 2005, **70**, 4323.
53 R.K. Dubey, N. Westerveld, E.J.R. Sudhölter, F.C. Grozema and W.F. Jager, *Org. Chem. Front*., 2016, **3**, 1481.
54 D. Inan, R.K. Dubey, N. Westerveld, J. Bleeker, W.F. Jager, and F.C. Grozema, *J. Phys. Chem. A*, 2017, **121**, 4633.
55 A. Colombo, C. Dragonetti, D. Roberto, R. Ugo, L. Falciola, S. Luzzati and D. Kotowski, *Organometallics,* 2011, **30**, 1279.
56 F. Nisic, A. Colombo, C. Dragonetti, E. Garoni, D. Marinotto, S. Righetto, F. De Angelis, M. G. Lobello, P. Salvatori, P. Biagini and F. Melchiorre, *Organometallics*, 2015, **34**, 94.
57 A. Colombo, F. Nisic, C. Dragonetti, D. Marinotto, I. P. Oliveri, S. Righetto, M. G. Lobello and F. De Angelis, *Chem. Commun*., 2014, **50**, 7986.
58 Y. Hirumi, K. Tamaki, T. Namikawa, K. Kamada, M. Mitsui, K. Suzuki, K. Kobayashi, *Chem. Asian J.* 2014, **9,** 1282.
59 K. Nishino, H. Yamamoto, K. Tanaka and Y. Chujo, *Org. Lett.,* 2016, **18**, 4064.
60 D. Pintossi, A. Colombo, M. Levi, C. Dragonetti, S. Turri and G. Griffini, *J. Mater. Chem. A,* 2017, **5**, 9067.
61 R.K. Dubey, N. Westerveld, F.C. Grozema, E.J.R. Sudhölter and W.F. Jager, *Org. Lett.,* 2015, **17**, 1882.
62 M. Sheik-Bahae, A. A. Said, T.-H. Wei, D. G. Hagan and E. W. van Stryland, *IEEE J. Quant. Electr.,* 1990, **26**, 760.
63 K. Kamada, K. Matsunaga, A. Yoshino and K. Ohta, *J. Opt. Soc. Am. B*, 2003, **20**, 529.
64 K. Kamada, Y. Iwase, K. Sakai, K. Kondo and K. Ohta, *J. Phys. Chem. C*, 2009, **113**, 11469.
65 Gaussian 09, Revision **D.01**, M. J. Frisch, G. W. Trucks, H. B. Schlegel, G. E. Scuseria, M. A. Robb, J. R. Cheeseman, G. Scalmani, V. Barone, B. Mennucci, G. A. Petersson, H. Nakatsuji, M. Caricato, X. Li, H. P. Hratchian, A. F. Izmaylov, J. Bloino, G. Zheng, J. L. Sonnenberg, M. Hada, M. Ehara, K. Toyota, R. Fukuda, J. Hasegawa, M. Ishida, T. Nakajima, Y. Honda, O. Kitao, H. Nakai, T. Vreven, J. A. Montgomery, Jr., J. E. Peralta, F. Ogliaro, M. Bearpark, J. J. Heyd, E. Brothers, K. N. Kudin, V. N. Staroverov, R. Kobayashi, J. Normand, K. Raghavachari, A. Rendell, J. C. Burant, S. S. Iyengar, J. Tomasi, M. Cossi, N. Rega, J. M. Millam, M. Klene, J. E. Knox, J. B. Cross, V. Bakken, C. Adamo, J. Jaramillo, R. Gomperts, R. E. Stratmann, O. Yazyev, A. J. Austin, R. Cammi, C. Pomelli, J. W. Ochterski, R. L. Martin, K. Morokuma, V. G. Zakrzewski, G. A. Voth, P. Salvador, J. J. Dannenberg, S. Dapprich, A. D. Daniels, Ö. Farkas, J. B. Foresman, J. V. Ortiz, J. Cioslowski, and D. J. Fox, Gaussian, Inc., Wallingford CT, 2009
66 A. Petersson, M. A. Al-Laham *J. Chem. Phys.*, 1991, **94**, 6081.
67 A.D. Becke, *J. Chem. Phys.,* 1993, **98**, 5648
68 S. Grimme, S. Ehrlich, L. Goerigk, *J. Comp. Chem*., 2011, **32**, 1456.
69 S. Miertus, E. Scrocco, J. Tomasi, *Chem. Phys.* 1981, **55**, 117.
70 M. Cossi, V. Barone, R. Cammi, J. Tomasi, *Chem. Phys. Lett.,* 1996, **255**, 327.

View Article Online
DOI: 10.1039/C8NJ03216E

Table of contents entry

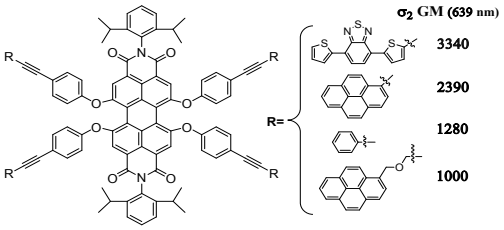

Perylenetetracarboxy-3,4:9,10-diimides with large TPA cross-sections.